Metabolite T_2 relaxation times decrease across the adult lifespan in a large multi-site cohort

Kathleen E. Hupfeld[a,b†], Saipavitra Murali-Manohar[a,b†], Helge J. Zöllner[a,b], Yulu Song[a,b], Christopher W. Davies-Jenkins[a,b], Aaron T. Gudmundson[a,b,c], Dunja Simičić[a,b], Gizeaddis Simegn[a,b], Emily E. Carter[d], Steve C. N. Hui[e,f,g], Vivek Yedavalli[a], Georg Oeltzschner[a,b], Eric C. Porges[d,h], and Richard A. E. Edden[a,b]

[a] Russell H. Morgan Department of Radiology and Radiological Science, Johns Hopkins University School of Medicine, Baltimore, MD, USA

[b] F. M. Kirby Research Center for Functional Brain Imaging, Kennedy Krieger Institute, Baltimore, MD, USA

[c] The Malone Center for Engineering in Healthcare, Johns Hopkins University, Baltimore, MD, USA

[d] Department of Clinical and Health Psychology, College of Public Health and Health Professions, University of Florida, Gainesville, Florida, USA

[e] Developing Brain Institute, Children's National Hospital, Washington, D.C. USA

[f] Department of Radiology, The George Washington University School of Medicine and Health Sciences, Washington, D.C. USA

[g] Department of Pediatrics, The George Washington University School of Medicine and Health Sciences, Washington, D.C. USA

[h] Center for Cognitive Aging and Memory, College of Medicine, University of Florida, Gainesville, Florida, USA

[†] Kathleen E. Hupfeld and Saipavitra Murali-Manohar contributed equally to this work.

Corresponding Author: Richard A. E. Edden, PhD
Russell H. Morgan Department of Radiology and Radiological Science
Johns Hopkins University School of Medicine, Baltimore, MD, USA 21287-0005
Email: raee2@jhu.edu

Running Title: T2 CHANGES WITH AGE

Word Count: 3,915 / 5,000 words

Figures and Tables: 8 / 10

Abstract (250 / 250 words)

Purpose

Relaxation correction is crucial for accurately estimating metabolite concentrations measured using *in vivo* magnetic resonance spectroscopy (MRS). However, the majority of MRS quantification routines assume that relaxation values remain constant across the lifespan, despite prior evidence of T_2 changes with aging for multiple of the major metabolites. Here, we comprehensively investigate correlations between T_2 and age in a large, multi-site cohort.

Methods

We recruited approximately 10 male and 10 female participants from each decade of life: 18-29, 30-39, 40-49, 50-59, and 60+ years old (n=101 total). We collected PRESS data at 8 TEs (30, 50, 74, 101, 135, 179, 241, and 350 ms) from voxels placed in white-matter-rich centrum semiovale (CSO) and gray-matter-rich posterior cingulate cortex (PCC). We quantified metabolite amplitudes using Osprey and fit exponential decay curves to estimate T_2.

Results

Older age was correlated with shorter T_2 for tNAA, $tCr_{3.0}$, $tCr_{3.9}$, tCho, Glx, and tissue water in CSO and PCC; r_s = -0.21 to -0.65, all p<0.05, FDR-corrected for multiple comparisons. These associations remained statistically significant when controlling for cortical atrophy. T_2 values did not differ across the adult lifespan for mI. By region, T_2 values were longer in the CSO for tNAA, $tCr_{3.0}$, $tCr_{3.9}$, Glx, and tissue water and longer in the PCC for tCho and mI.

Conclusion

These findings underscore the importance of considering metabolite T_2 changes with aging in MRS quantification. We suggest that future 3T work utilize the equations presented here to estimate age-specific T_2 values instead of relying on uniform default values.

Keywords: T_2 relaxation times, TE series, magnetic resonance spectroscopy (MRS), metabolites, healthy aging

1. Introduction

Understanding brain changes across the healthy adult lifespan is critical for preserving brain health in the quickly aging global population and uncovering possible mechanisms of age-related neurological disease. Proton magnetic resonance spectroscopy (^{1}H MRS) is the only methodology that allows non-invasive measurements of endogenous brain metabolite concentrations. However, MRS data are often acquired at echo times (TEs) that are non-negligible compared to metabolite transverse relaxation rates (T_2). This results in T_2-weighting of the signal, such that metabolite amplitude changes associated with normal aging might be caused by changes in relaxation but misinterpreted as changes in metabolite concentration. This confound exists even for short-TE MRS, but is particularly a concern for *J*-difference-edited MRS[1], which relies on TEs of >65 ms (constrained by the duration of frequency-selective editing pulses and the J-evolution of target metabolites). Thus, recent consensus[1–3] suggests that it is critical to address the confound of T_2 relaxation (including for reference signals), particularly in studies of aging and neurodegeneration. However, despite this, most MRS quantification procedures (likely incorrectly) use static reference values, which assume that metabolite T_2 relaxation remains constant across the adult lifespan.

Prior work has reported varied relationships between age and T_2, primarily for the singlet resonances total *N*-acetyl aspartate (tNAA), creatine (tCr), and choline (tCho). A majority of prior work at 3 and 4 T has reported shorter metabolite T_2s with older age both for metabolites[4–7] and tissue water[4,7]. A few studies[8,9] at 1.5 T have reported the opposite effect of longer metabolite T_2s with older age; however, one of these studies[9] was complicated by overlap among water and metabolite signals, and the other[8] examined only the frontal lobe and included only males in the sample. One study[10], also at 1.5 T, found longer NAA T_2 in the centrum semiovale of older adults; however, this study utilized a linewidth-based approach which has not been validated or used again since publication in 2005. With the exception of work by Brooks and colleagues[8], each of these prior studies involved comparison of discrete age groups (young versus older

adults) rather than continuous sampling across the adult lifespan, and each used small sample sizes (all $n < 20$ per age group, with the exception of work by Deelchand and colleagues[4] which included 32 young and 26 older adults). Therefore, in the present study, we leveraged a large, multi-site cohort in order to more comprehensively investigate whether metabolite and tissue water T_2 values differ across the normal adult lifespan, and to provide statistical models for calculating age-specific T_2 values for future integration into MRS quantification procedures.

2. Methods

2.1 Participants

101 healthy adults provided written informed consent to participate at one of two sites: the Johns Hopkins University School of Medicine ($n = 51$) and the University of Florida ($n = 50$). The sample included approximately 10 females and 10 males from each of the following decades: 18–29, 30–39, 40–49, 50–59, and 60+ years (Table 1). The Johns Hopkins University and University of Florida Institutional Review Boards approved all study procedures. Participants first completed the Montreal Cognitive Assessment (MoCA)[11], followed by a 1-hour MRI protocol. Of note, four individuals scored below the cut-off score of 23 out of 30 (i.e., indicative of possible mild cognitive impairment[12]). However, MoCA score was not an *a priori* exclusion criterion for this study. Moreover, each of these individuals scored 22 (just below the cut-off), and 3 of these 4 reported that English was not their primary language which can negatively impact MoCA performance[13] (and it was not feasible to conduct the MoCA in a language other than English). Therefore, we presumed that cognitive impairment was not likely and opted to retain these individuals in the cohort and statistical analyses.

Table 1. Participant Demographics

Variable	18-29 years	30-39 years	40-49 years	50-59 years	60+ years
Sex, #	10 F, 13 M	10 F, 10 M	10 F, 10 M	9 F, 9 M	11 F, 9 M
Age, Mean (SD), [Min, Max], years	24.2 (3.3) [18.7, 29.8]	35.0 (2.9) [30.3, 39.9]	44.2 (3.0) [40.0, 49.2]	55.0 (2.9) [50.2, 59.8]	67.5 (4.1) [60.8, 75.4]
MoCA, Mean (SD)[a] [Min, Max]	27.9 (2.0) [23, 30]	28.0 (2.3) [23, 30]	27.6 (2.5) [22, 30]	26.3 (1.8) [23, 29]	27.7 (2.5) [22, 30]

[a] One point was added to the MoCA score for n = 9, as these individuals reported having completed 12 years of education or less[11].

2.2 MRS Acquisition

All scans were performed using a 32-channel head coil on either the Johns Hopkins University 3 T Philips dStream Ingenia Elition MRI scanner or the University of Florida 3 T Philips MR7700 MRI scanner. For voxel positioning, we first collected a T_1-weighted structural MRI scan using the following parameters: MPRAGE, TR/TE 2000 ms/2 ms, flip angle 8°, slice thickness 1.0 mm, 150 slices, voxel size 1 mm^3 isotropic, total time 2 min 46 sec. Next, we acquired TE series data from two 30 x 26 x 26 mm^3 voxels: the white matter (WM) rich centrum semiovale (CSO) and the gray matter (GM) rich posterior cingulate cortex (PCC; Figure 1). Scan parameters for the TE series included: PRESS localization, TR 2000 ms, 8 logarithmically-spaced TEs 30, 50, 74, 101, 135, 179, 241, and 350 ms, 24 transients per TE sampled at 2000 Hz with 1024 points, and CHESS water suppression (115 Hz bandwidth). Within each series, the TE steps were neither interleaved nor randomized. We also collected a separate series of unsuppressed water reference data at each of the 8 TEs with the same parameters, but with 2 transients per TE and no water suppression. Of note, these voxel sizes and locations were selected to match those collected in our recent cohort of short-TE PRESS metabolite data in 102 individuals ranging from their 20s to their 60s[14].

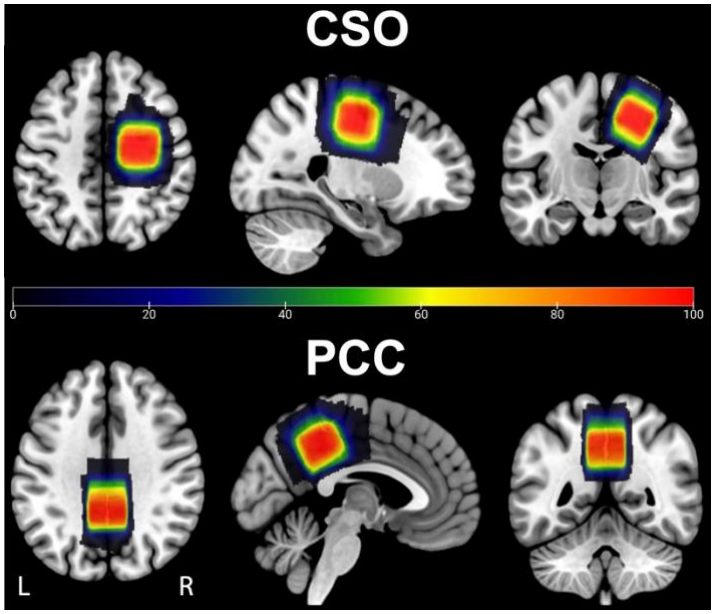

Figure 1. Voxel Placement. TE series data were acquired from the centrum semiovale (CSO) and posterior cingulate cortex (PCC). Each participant's native space binary voxel mask for their CSO and PCC voxels was normalized to standard (MNI) space and overlaid onto the spm152 template. Warmer colors indicate areas of greater overlap between participants (color bar = number of subjects overlapped).

2.2 MRS Data Processing

MRS data were analyzed within MATLAB R2021b using the open-source analysis toolbox Osprey (v2.5.0; https://github.com/schorschinho/osprey/)[15]. All analysis procedures followed consensus-recommended guidelines[1,3]. Briefly, analysis steps included: loading the vendor-native raw data (which had already been coil-combined, eddy-current-corrected, and averaged on the scanner at the time of data collection), removing the residual water signal using a Hankel singular value decomposition (HSVD) filter[16], and modeling the metabolite peaks at each TE separately as described previously[15,17] using TE-specific custom basis sets. The basis sets were simulated by the MRSCloud tool[18] (https://braingps.mricloud.org/mrs-cloud). MRSCloud using a localized 2D density-matrix simulation of a 101 x 101 spatial grid (voxel size 30 x 30 x 30 mm^3; field of view 45 x 45 x 45 mm^3) and vendor-specific refocusing pulse shape, duration, and sequence timings based on the MATLAB simulation toolbox FID-A[19]. The basis sets consisted of 18 basis functions: ascorbate (Asc), aspartate (Asp), creatine (Cr), negative creatine methylene (-$CrCH_2$), gamma-aminobutyric acid (GABA), glycerophosphocholine (GPC),

glutathione (GSH), glutamine (Gln), glutamate (Glu), lactate (Lac), myo-inositol (mI), *N*-acetyl aspartate (NAA), *N*-acetyl aspartyl glutamate (NAAG), phosphocholine (PCh), phosphocreatine (PCr), phosphoethanolamine (PE), scyllo-inositol (sI), and taurine (Tau), as well as 5 macromolecule signals (MM09, MM12, MM14, MM17, MM20) and 3 lipid signals (Lip09, Lip13, Lip20) included as parameterized Gaussian functions[17].

We extracted amplitudes for 6 metabolites of interest: tNAA, tCho, $tCr_{3.0}$ (Cr + PCr), $tCr_{3.9}$ (Cr + PCr - ($-CrCH_2$)), mI, and Glx (Glu + Gln). We multiplied each metabolite amplitude by Osprey's internal *MRSCont.fit.scale* factor for each TE and participant to make the metabolite amplitudes directly comparable across TEs. This scaling factor is applied to the data to ensure an optimal dynamic range between the data and basis set during modeling. It is defined as the ratio of the maximum of the real part of the data and the basis set in the model range. Next, we used *lsqcurvefit* in MATLAB to fit monoexponential T_2 decay functions to the TE series metabolite amplitudes (Equation 1) in order to obtain the T_2 decay constant and an R^2 value of model fit for each participant for each metabolite.

$$y_i = A_i * e^{\left(-\frac{TE}{T_2 i}\right)} \quad \textbf{[1]}$$

In Equation 1, y_i represents the metabolite amplitude, A_i is a scaling constant, and T_{2i} is the relaxation time to be calculated for the i^{th} subject. Lastly, we created a binary mask of the two MRS voxels in subject space, co-registered these masks to each participant's T_1-weighted structural scan, and segmented the structural scans using SPM12[20], in order to calculate the volume fractions of white matter (fWM), gray matter (fGM), and cerebrospinal fluid (fCSF) in each participant's voxels in subject space (for use in statistical models to control for cortical atrophy and for estimation of tissue water T_2).

We then repeated a similar procedure for tissue water. To estimate the water amplitudes, the unsuppressed water data at each TE was modeled using a linear combination

model with a simulated water signal[18]. We used MATLAB's *lsqcurvefit* to fit a biexponential decay function (Equation 2) to obtain tissue water T_2 and R^2 values for each participant.

$$y_i = A_i * e^{\left(-\frac{TE}{T_{2wi,tissue}}\right)} * 0.4211 * (1 - fCSF) + A_i * e^{\left(-\frac{TE}{T_{2wi,CSF}}\right)} * 0.5789 * fCSF \quad \textbf{[2]}$$

In Equation 2, y_i represents the water amplitude, A_i is a scaling constant, $T_{2wi,tissue}$ is the tissue water relaxation time, and $T_{2wi,CSF}$ is the CSF water relaxation time to be calculated for the i^{th} subject. fCSF is the fraction of CSF within the voxel for the i^{th} subject; 0.4211 weights the first term by the approximate molal concentration of water for non-CSF tissue (40/(40+55)), and 0.5789 weights the second term by the approximate molal concentration of water for CSF (55/(40+55)). The A_i and $T_{2wi,tissue}$ terms were unconstrained, and the $T_{2wi,CSF}$ term was constrained to the range of 50–3000 ms[21–23]. A data acquisition error occurred at the University of Florida site for the water data; therefore, we included only the Johns Hopkins University participants (n = 51) in statistical analyses of the water T_2 data.

2.3 Statistical Analyses

We conducted all statistical analyses using R 4.3.2[24] within RStudio[25]. First, we calculated descriptive statistics (mean, standard deviation) by age group for the T_2 values for each of the 6 metabolites of interest and tissue water. Next, we examined the correlation between T_2 and age for each metabolite and voxel separately. As multiple variables did not satisfy the Pearson correlation normality assumption (Shapiro test $p < 0.05$), we instead report nonparametric Spearman correlations. To account for multiple comparisons, we applied the Benjamini-Hochberg false discovery rate (FDR) correction to the p-values for each voxel[26]. Secondly, we ran a series of linear models, setting each metabolite T_2 as the outcome variable and age as the predictor: $T_2 = \beta_0 + \beta_1*(\text{Age-30})$. We centered age around 30 years, so that the intercept (β_0) from this model would represent the predicted metabolite T_2 value at 30 years old, and the slope (β_1) would represent the change in T_2 for each year of age. The aim of this model was to provide an equation to calculate predicted T_2 value for a given metabolite given the age

of a participant. As a follow-up analysis, we reran each of these linear models controlling for the potential effects of cortical atrophy with aging: $T_2 = \beta_0 + \beta_1*(Age-30) + \beta_2*Tissue$. As in our recent work examining metabolite T_1 changes with aging[27], we calculated cortical atrophy as the relative tissue fraction within the voxel, fGM / (fWM + fGM). The purpose of this follow-up model was to ensure that cortical atrophy effects were not a major contributing factor to the observed T_2 relationships with age.

In addition, we conducted a series of paired t-tests (followed by FDR correction of the *p*-values[26]) to examine differences in metabolite T_2 values between the CSO and PCC voxels. We also computed one linear mixed effects model per metabolite in which we set T_2 (across both the CSO and PCC voxels) as the outcome variable, age, voxel, and the interaction of age with voxel as the predictors, and a random intercept (u_i) for each subject: $T_2 = \beta_0 + \beta_1*(Age-30) + \beta_2*Voxel + \beta_3*(Age-30)*Voxel + u_i$. The primary aim of this model was to test for any Age*Voxel interaction effects (i.e., whether the age slope differed by brain region in any cases). The linear mixed effects model and random subject intercepts were necessary because this modeling approach structured the data as 'repeated measures' in which each participant had two measurements (CSO T_2 and PCC T_2).

3. Results

3.1 Data Quality

Creatine (Cr) linewidths were well within the range of consensus-recommended standards (i.e., < 13 Hz for 3 T^3) for all spectra except one individual's CSO voxel (33-year-old male, Cr linewidth = 14.1 Hz). In addition, for one participant (19-year-old male), the PCC voxel was mistakenly positioned at the wrong location. Thus, these datasets (1 CSO and 1 PCC) were excluded before any statistical analyses. Additional consensus-recommended data quality metrics are presented in Appendix A. Example single-subject spectra at each TE and decay

functions for each metabolite are presented in Figure 2. The mean R^2 value across the whole cohort for the goodness of fit of the T_2 decay model was ≥0.80 for each of the 6 metabolites of interest and tissue water. Table 2 presents descriptive statistics by age group for the T_2 values.

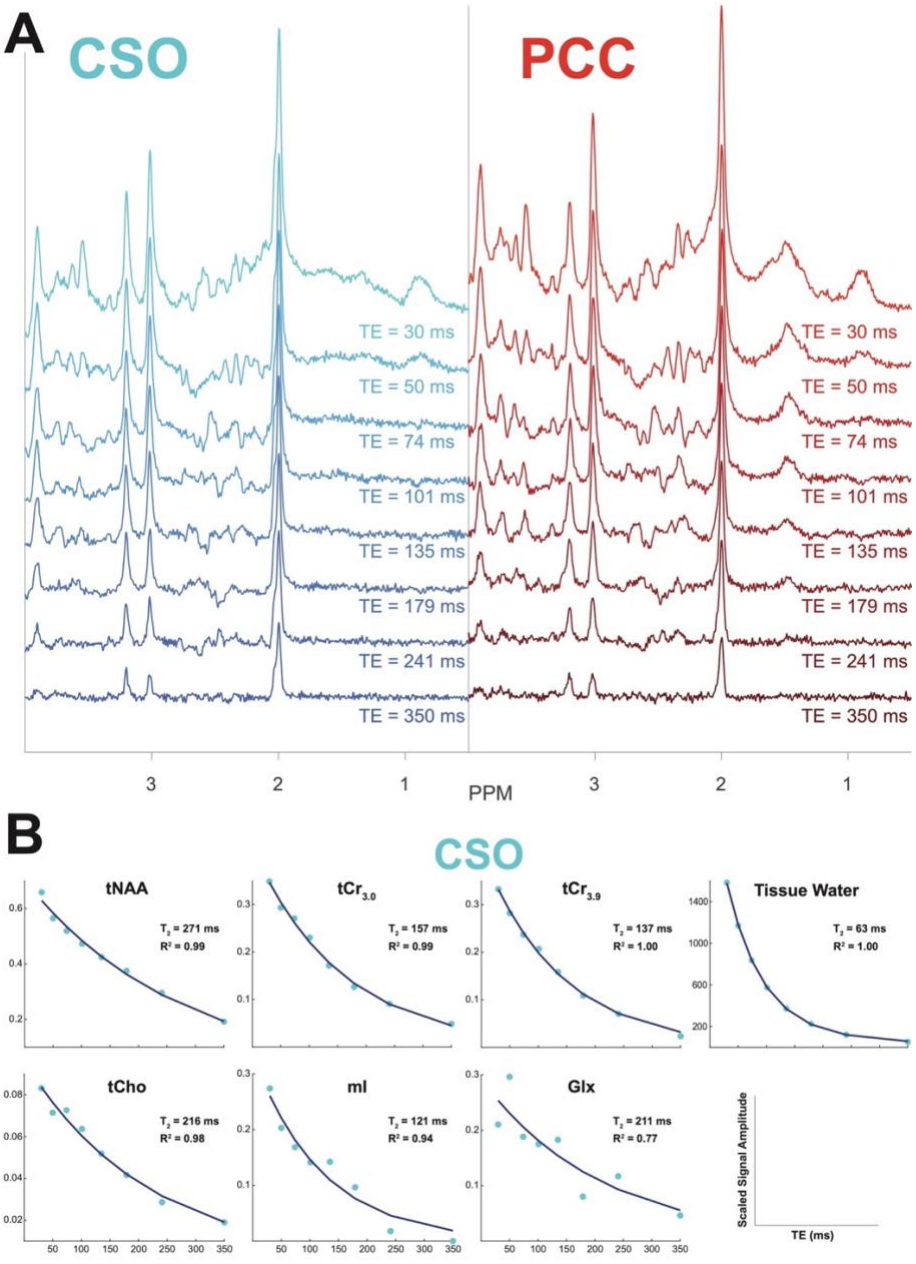

Figure 2. Single-Subject Example Spectra and CSO T_2 Decay. A PRESS spectra for each of the 8 TEs for the CSO (left) and PCC (right) voxels for a representative subject (48-year-old female). This representative subject was determined by averaging the R^2 values of model fit across the 6 metabolites and tissue water for each person in the Johns Hopkins cohort (as water data were unavailable for University of Florida subjects) and then taking the group median of this average R^2 value. **B** Example T_2 decay plots for the 6 metabolites and tissue water from the CSO voxel for the same representative subject. Blue points represent the metabolite amplitude at each TE, and the dark blue line represents the calculated T_2 decay curve.

Table 2. T_2 Descriptive Statistics by Age Group

CSO Voxel					
Metabolite	**18-29 years** Mean (SD)	**30-39 years** Mean (SD)	**40-49 years** Mean (SD)	**50-59 years** Mean (SD)	**60+ years** Mean (SD)
tNAA	298.9 (22.5)	283.8 (24.3)	267.9 (24.2)	267.9 (24.6)	260.6 (23.8)
$tCr_{3.0}$	159.5 (10.6)	153.0 (8.8)	147.7 (11.5)	148.3 (8.9)	147.9 (8.6)
$tCr_{3.9}$	145.0 (10.7)	133.9 (16.2)	133.0 (10.3)	133.9 (8.6)	132.9 (9.3)
tCho	230.1 (18.6)	216.3 (24.4)	203.0 (19.7)	204.5 (17.7)	207.8 (19.7)
mI	146.7 (14.0)	141.5 (17.2)	132.7 (11.7)	144.8 (16.0)	140.6 (19.0)
Glx	206.1 (40.6)	213.7 (36.7)	186.3 (29.6)	195.6 (42.1)	181.5 (30.3)
Tissue Water[a]	64.8 (2.1)	64.1 (2.3)	62.7 (2.6)	62.5 (3.1)	62.4 (2.5)
PCC Voxel					
Metabolite	**18-29 years** Mean (SD)	**30-39 years** Mean (SD)	**40-49 years** Mean (SD)	**50-59 years** Mean (SD)	**60+ years** Mean (SD)
tNAA	255.2 (22.6)	237.1 (12.8)	224.0 (15.3)	221.1 (16.7)	215.6 (14.7)
$tCr_{3.0}$	155.5 (8.9)	149.6 (7.8)	144 (8.6)	145.3 (5.8)	145.8 (8.5)
$tCr_{3.9}$	131.1 (9.1)	126.4 (5.2)	125.8 (9.6)	123.6 (7.4)	127.6 (10.0)
tCho	258.2 (25.2)	240.3 (13.3)	221 (15.9)	224.2 (20.2)	228.0 (20.3)
mI	166.8 (15.0)	157.1 (13.7)	157.5 (14.2)	158.0 (13.6)	159.5 (16.3)
Glx	166.8 (19.2)	156.7 (21.6)	164.8 (29.3)	162.9 (23.8)	147.6 (31.2)
Tissue Water[a]	54.8 (4.0)	55.2 (2.5)	52.1 (2.5)	49.7 (5.9)	50.7 (2.7)

Note. This table lists T_2 values in ms for the 6 metabolites and tissue water.

[a] Tissue water includes only the n = 51 Johns Hopkins subjects.

3.2 T_2 Relationships with Age

Older age was significantly correlated with shorter T_2 values for tNAA, $tCr_{3.0}$, $tCr_{3.9}$, tCho, Glx, and tissue water in both the CSO and PCC; Spearman r = -0.21 to -0.65, $p < 0.05$, FDR-corrected for multiple comparisons (Figure 3; Table 3). Age was most strongly correlated with tNAA T_2. Age did not correlate with mI T_2 for either voxel.

Table 3. T_2 Correlations with Age

Metabolite	CSO		PCC	
	r_s	$p_{FDR\text{-}corr}$	r_s	$p_{FDR\text{-}corr}$
tNAA	-0.46	< 0.001***	-0.65	< 0.001***
$tCr_{3.0}$	-0.37	< 0.001***	-0.43	< 0.001***
$tCr_{3.9}$	-0.34	0.001**	-0.21	0.047*
tCho	-0.38	< 0.001***	-0.51	< 0.001***
mI	-0.07	0.477	-0.17	0.095
Glx	-0.34	0.001**	-0.24	0.022*
Tissue Water[a]	-0.30	0.035*	-0.46	0.001**

Note. This table presents the Spearman r values and FDR-corrected *p*-values for the correlation of age with metabolite T_2 in the CSO and PCC voxels separately; *p<0.05, **p<0.01, ***p<0.001.

[a] Tissue water includes only the n = 51 Johns Hopkins subjects.

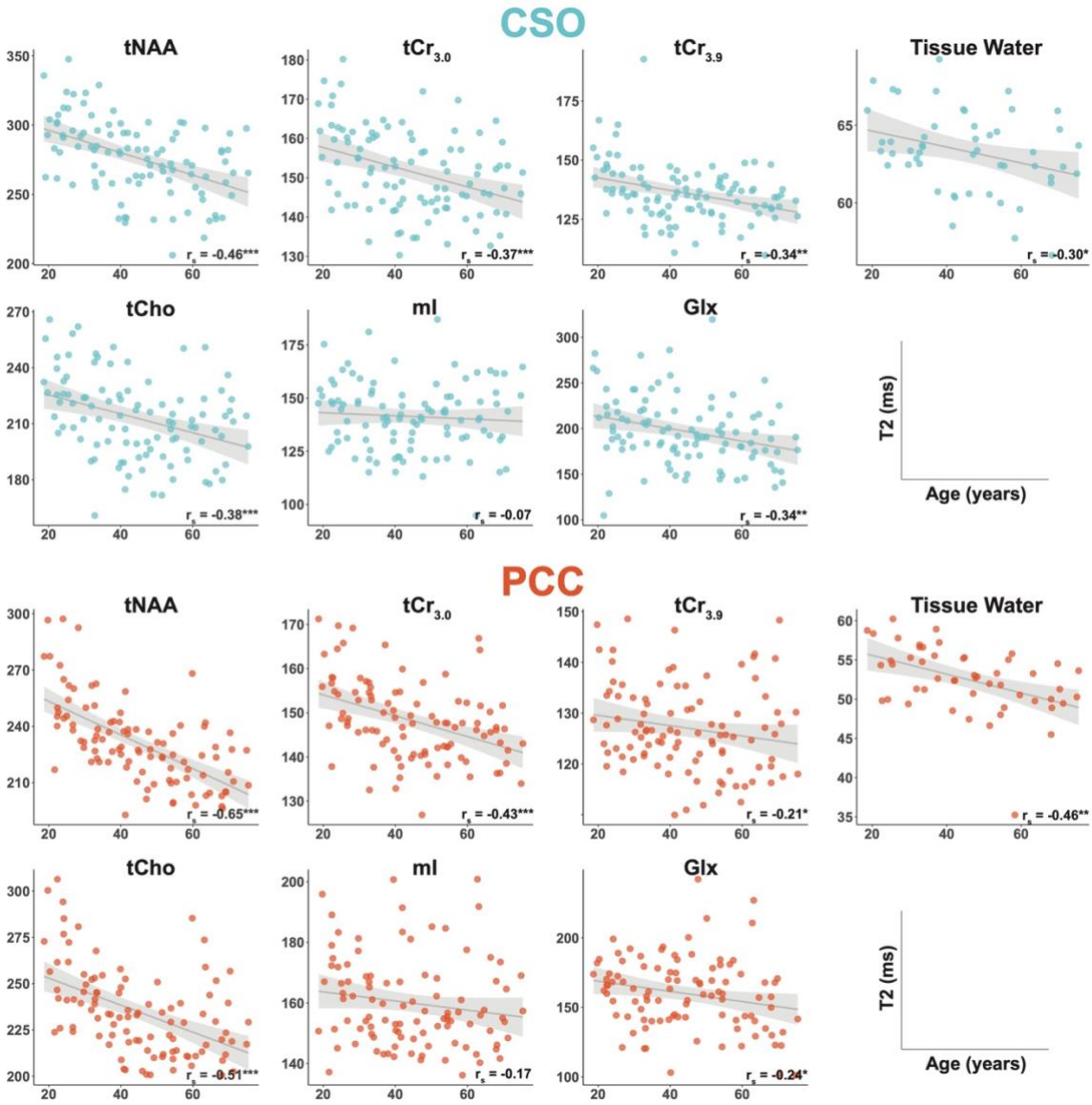

Figure 3. Metabolite T_2 Correlations with Age. T_2 correlations with age are shown for the CSO (above, blue) and PCC (below, orange). Each point represents one participant. The bottom right corner of each

plot indicates the Spearman correlation coefficient (r_s) and statistical significance of the FDR-corrected *p*-value for the correlation, **p*<0.05, ***p*<0.01, ****p*<0.001. The gray line and shading represent the linear model and 95% confidence interval for the model using age to predict T_2 (produced using the *geom_smooth* function in R).

Next, we fit linear models to predict T_2 using age for each metabolite and voxel combination: $T_2 = \beta_0 + \beta_1*(\text{Age}-30)$; Table 4. As we centered age around 30 years old, the intercept (β_0) represents the predicted T_2 value for each metabolite at 30 years of age (as opposed to age 0 which would represent an unhelpful extrapolation). The slope (β_1) represents the change in the predicted value of T_2 for each year of life. For example, for tNAA in the CSO, the predicted T_2 value for an individual age 30 years would be: $T_2 = 288.27 + (30-30)*-0.81 = 288.27$ ms, while the predicted T_2 value for an individual age 50 years would be $T_2 = 288.27 + (50-30)*-0.81 = 272.07$ ms. (Note that these predicted T_2 values also correspond to the gray linear model lines plotted in Figure 3). The slope and intercept values listed in Table 4 can thus be utilized to calculate a predicted T_2 for any age in a WM- or GM-rich voxel. Table 4 only includes slopes for the metabolites which were significantly correlated with age.

Table 4. Model Coefficients for Estimating T_2

Metabolite	CSO		PCC	
	Intercept	Slope (β_1)	Intercept	Slope (β_1)
tNAA	288.27	-0.81	244.35	-0.89
$tCr_{3.0}$	155.21	-0.25	151.67	-0.24
$tCr_{3.9}$	139.88	-0.26	128.53	-0.10
tCho	220.32	-0.51	245.66	-0.73
mI	142.39		162.13	
Glx	206.54	-0.68	165.20	-0.37
Tissue Water[a]	64.11	-0.05	54.38	-0.12

Note. This table presents the intercept and slope (β_1) values for the linear model using age to predict T_2 values: $T_2 = \beta_0 + \beta_1*(\text{Age}-30)$. Slope is listed only for the metabolites which were significantly correlated with age. As Age is centered around 30 years in the equation, the intercept (β_0) represents the predicted T_2 value for each metabolite at Age = 30 years. The slope (β_1) represents the change in the predicted value of T_2 for each 1-year increase in age beyond 30. This model can be used in future work to predict a T_2 value for a given age for these metabolites.

[a] Tissue water includes only the *n* = 51 Johns Hopkins subjects.

Older age was significantly correlated with greater cortical atrophy (calculated as fGM / (fWM + fGM)) in the PCC (r_s = -0.25; *p* = 0.010) but not the CSO (r_s = -0.04; *p* = 0.680). As a

follow-up to the linear models presented in Table 4, we reran each model controlling for cortical atrophy with aging: $T_2 = \beta_0 + \beta_1*(\text{Age-30}) + \beta_2*\text{Tissue}$ (see Supplementary Table B1). Including this metric of cortical atrophy in the model did not change the statistical significance of any T_2 relationships with age, with the exception of $tCr_{3.9}$ in the PCC (for which the age-T2 relationship became non-significant, $p = 0.094$). Independent of the associations between age and T_2, greater cortical atrophy was significantly associated with longer metabolite T_2 values for tNAA, $tCr_{3.0}$, and $tCr_{3.9}$ (CSO only), as well as mI and tissue water (CSO and PCC).

3.2 T_2 Differences by Voxel

Paired t-tests revealed differences in T_2 values by voxel for all metabolites (as shown in Figure 4). T_2 values were higher in the CSO than in the PCC for tNAA, $tCr_{3.0}$, $tCr_{3.9}$, Glx, and tissue water, and lower in the CSO for tCho and mI.

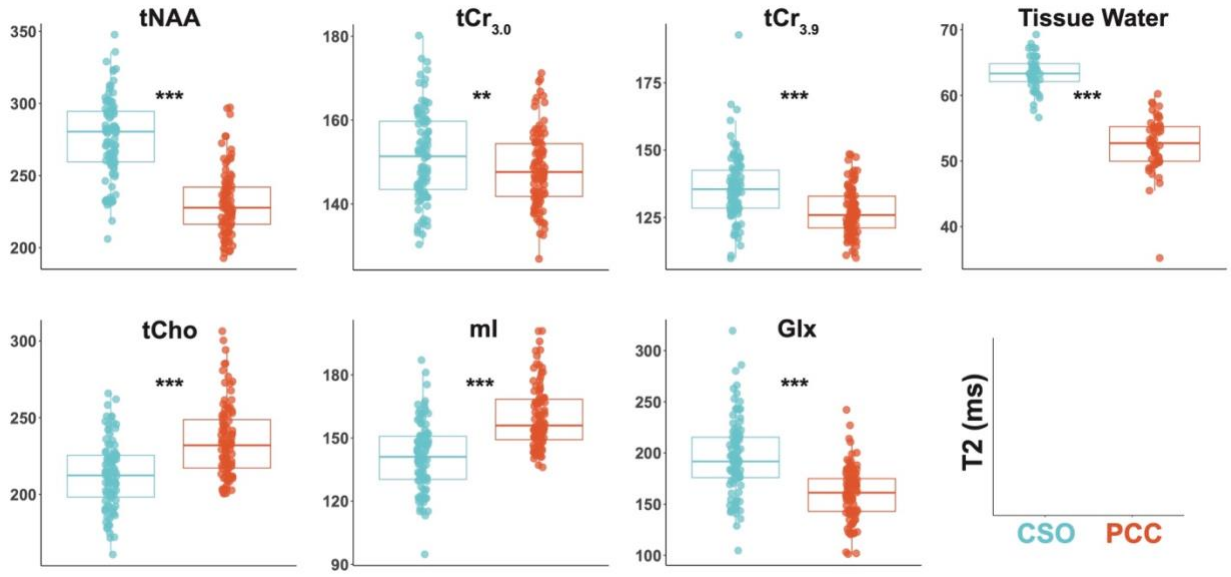

Figure 4. Metabolite T_2 Differences by Voxel. T_2 differences by voxel are shown for the CSO (blue) and PCC (orange). Each point represents one participant. The asterisks indicate the statistical significance of the FDR-corrected *p*-value for the paired t-test, *p<0.05, **p<0.01, ***p<0.001.

As a follow-up analysis, we computed one linear mixed effects model per metabolite (across both the CSO and PCC) to test whether the age slope differed by brain region for any metabolites or tissue water. The Age*Voxel interaction was significant only for tissue water

(p=0.007), indicating that, in all but one case, the relationship of age with T_2 did not differ based on brain region (Supplementary Table B2). However, for tissue water, the relationship of age with T_2 was stronger for the PCC than the CSO.

4. Discussion

Here we present the largest analysis to date examining metabolite and tissue water T_2 changes across the healthy adult lifespan. Among 101 adults ages 18-75 and across two sites, metabolite and tissue water T_2 values in both the CSO and PCC were generally significantly shortened with age, even when controlling for age-related cortical atrophy. Moreover, T_2 values were longer in the CSO, with the exception of tCho and mI which exhibited longer T_2 in the PCC. Taken together, these results align with the majority of prior work which also reported T_2 declines with normal aging (but in much smaller cohorts). Moreover, the finding of T_2 differences based on age and brain region highlights the importance of measuring subject-level T_2 during data acquisition or employing estimation methods (such as the statistical models provided here) for calculating age- and region-appropriate T_2 values.

Older age was correlated with shorter metabolite T_2 values for tNAA, $tCr_{3.0}$, $tCr_{3.9}$, tCho, Glx, and tissue water in both the CSO and PCC. This aligns with most prior research in smaller samples which similarly found shorter tNAA, tCr, tCho, and tissue water T_2s with older age[4–7]. As also seen in these prior studies, we identified the strongest age association for tNAA. Most prior reports did not examine Glx. Deelchand and colleagues (2020) reported reduced mI T_2 in CSO and PCC in older age, whereas we did not find an association between mI T_2 and age. However, it should be noted that Deelchand and colleagues[4] compared two age groups (rather than treating age as a continuous variable), and their older cohort (ages 70-83 years) extended beyond our upper age range.

The specific mechanisms underlying these observed T_2 changes with aging remain unclear. With the exception of $tCr_{3.9}$ in the PCC, each of the identified T_2 associations with age

remained statistically significant when controlling for cortical atrophy, suggesting that age-related atrophy is not a major factor in these findings. Instead, as metabolites are largely intracellular (glial or neuronal)[28], their T_2 relaxation times are likely influenced by changes in the cellular microenvironment[4], i.e. cellular morphology, metabolism, or myelination[4,7]. It is well established that neurons undergo morphological changes during aging—such as reduction in soma size and loss or regression of dendrites and dendritic spines[29]— alongside a parallel metabolic shift in astrocytes associated with increased neuroinflammatory response and changes in oxidative metabolism[30,31]. Furthermore, degeneration of myelin sheath[32] and loss of axonal fiber[32] with advancing age, accompanied by debris (e.g., protein aggregates) and degraded myelin accumulation[33,34] reported in white matter and further supported by *in vivo* diffusion tensor imaging[35,36].

The observed T_2 changes could also be influenced by the gradual deposition of iron, particularly Fe^{3+}, in the brain with aging. Although iron is present in the brain in multiple forms, the intracellular non-heme iron (i.e., ferritin) in tissue is thought to cause dephasing of the proton spins and thus a faster T_2 decay[37]. Several studies observed a strong linear correlation between iron concentrations and transverse relaxation (R_2)[38] values both *in vivo* and in post-mortem healthy and Alzheimer's disease brain tissue[37], suggesting that faster T_2 relaxation is related to age-related iron deposition[39]. Whilst the precise contribution of each of these mechanisms is unclear, the observed age relationships suggest that T_2 measurements are sensitive to various parallel changes in the cellular environment[7].

In this dataset, T_2 relaxation times were predominantly longer for tNAA, $tCr_{3.0}$, $tCr_{3.9}$, Glx, and tissue water in the WM-rich CSO, whereas tCho and mI exhibited longer T_2 in the GM-rich PCC. There is relatively limited literature considering GM/WM differences in metabolite T_2, and this prior work differs in voxel location, cohort, acquisition and quantification methodology, and statistical approach. Of the seven references we identified[6,40–45], five reported longer T_2 for NAA in WM as we did[6,40–42,45], while one revealed no significant tissue effect[43] and one showed the

reverse effect[44]. For $tCr_{3.0}$, three references found our result of longer T_2 in WM[6,41,42], three showed no difference[40,43,45], and the same study showed the reverse effect[44]. Only a few studies have measured T_2s of $tCr_{3.9}$ or Glx. For $tCr_{3.9}$, one paper showed longer T_2s in WM[45] (as we found) and one no difference[42]; for Glx, one study that separated Glx as Glu and Gln with J-PRESS found no differences by tissue type in the major component, Glu[42]. For tCho, four studies found no difference[40,41,43,45], two found longer T_2 in GM[42,44] (as we did), and one longer T_2 in WM[6]. T_2 of mI remains less investigated, but the two studies that measured mI T_2 also found longer T_2 in GM[42,44]. For tissue water, GM is generally found to have longer T_2 values than WM in multi-echo MRI experiments[46–48], although the extent to which CSF confounds this result depends on resolution. Regional T_2 differences may relate to greater micro- and macro-structural organization in myelinated WM compared to GM[49]; however, further work is needed to fully understand the mechanisms that govern metabolite T_2 relaxation.

We recently performed a meta-regression analysis of 75 manuscripts[50] containing 629 unique values to derive a general predictive T_2 model, with linear factors for: metabolite, field strength, species, tissue, pulse sequence, and Carr-Purcell Meiboom-Gill filter. The average bias between the (30-year-old intercept) values reported in the present study and the model predicted values was +9 ms (i.e., on average the model predicts shorter T_2s than measured here). The average absolute difference was 23 ms which is smaller than the average absolute difference between the predicted model and the T_2 training dataset (42 ms). On this basis, we assert that our results are consistent with the diverse T_2 literature.

2D modeling of interrelated MRS data has recently gained interest in the MRS community[51–53]. Most notably, it was found that 2D modeling of synthetic multi-TE MRS data with overlapping peaks led to improved precision due to improved model parsimony achieved through reparametrization[51]. Applying 2D modeling to our *in vivo* datasets may improve the T_2 estimation of the metabolites reported here and could potentially allow for the T_2 estimation of additional low-SNR metabolites. However, it will also require careful reparameterization of the T_2

relaxation constants, lineshape estimates, and baseline terms, which will be part of future studies.

There are several limitations to this work. First, we acknowledge that our T_2 measurement here is a complex mix of pure T_2 and some inhomogeneous broadening factors that are not fully refocused by the two PRESS spin echoes. The goal of the present work was to improve the accuracy of T_2 relaxation correction in quantification procedures by understanding age effects on our measure of T_2 (rather than to accurately measure pure T_2). Second, future work could expand upon the age range to include those younger than 18 and older than 70 years, as well as targeting both normal and pathological aging (e.g., Alzheimer's and other neurodegenerative diseases). Given the potential of T_2 to reflect both micro- and macrostructural organization, the measure may show utility as an early indicator of these changes, as suggested by Kirov and Tal[54]. Though this was a large cohort with systematic recruitment across the adult lifespan, we only enrolled a few individuals older than age 70 years (the timeframe at which aging effects drastically accelerate). Lastly, we were limited to collecting only two voxels (WM-rich CSO and GM-rich PCC); however, prior evidence suggests that neurochemical changes with aging are highly region-dependent[55], and therefore future work might consider probing T_2 changes in other brain regions, or across the entire brain.

5. Conclusions

Consistent with prior literature, in a large multi-site cohort sampled systematically across the adult lifespan, we identified a clear age-related decrease in T_2 for multiple metabolites and tissue water, as well as differences in T_2 between the WM-rich CSO and GM-rich PCC. Together, these findings highlight potential changes in the brain's cellular microenvironment with normal aging and underscore the critical importance of considering metabolite T_2 differences across the adult lifespan in MRS quantification procedures. We suggest that future MRS work

leverage the models presented here to estimate age- and region-specific T_2 values instead of relying on uniform default values.

Competing Interests

All authors declare that they have no competing interests.

Author Contributions

KH processed all data, conducted all statistical analyses, prepared all figures and supplemental material, and prepared the manuscript. SM contributed to protocol development, manuscript writing and led all revisions of the manuscript. HZ contributed to MRS data processing, and developed Osprey code for the analysis. YS and EC made significant contributions to data collection. CDJ generated the spectra figure and contributed to interpretation of results. AG, DS, and GS contributed to interpretation of results and drafted parts of the Discussion. VY reviewed all structural scans to assess data quality and check for incidental findings. SH set up the scan protocol and oversaw data quality control. GO, EP, and RAE designed the project and led interpretation of the results. All authors participated in revision of the manuscript.

Funding

This work was supported by grants from the National Institute on Aging (K00 AG068440 to KH, R00 AG062230 to GO, and K99 AG080084 to HZ) and grants from the National Institute of Biomedical Imaging and Bioengineering (R21 EB033516 to GO, R01 EB023963 to RE, R01 EB016089 to RE, and P41 EB031771).

Acknowledgements

The authors also wish to thank all of the participants who volunteered their time, as well as support staff at both MRI centers, without whom this project would not have been possible.

References

1. Choi IY, Andronesi OC, Barker P, et al. Spectral editing in 1H magnetic resonance spectroscopy: Experts' consensus recommendations. *NMR Biomed*. 2021;34(5):e4411.

2. Near J, Harris AD, Juchem C, et al. Preprocessing, analysis and quantification in single-voxel magnetic resonance spectroscopy: experts' consensus recommendations. *NMR Biomed*. 2021;34(5). doi:10.1002/nbm.4257

3. Wilson M, Andronesi O, Barker PB, et al. Methodological consensus on clinical proton MRS of the brain: Review and recommendations. *Magn Reson Med*. 2019;82(2):527-550.

4. Deelchand DK, McCarten JR, Hemmy LS, Auerbach EJ, Eberly LE, Marjańska M. Changes in the intracellular microenvironment in the aging human brain. *Neurobiol Aging*. 2020;95:168-175.

5. Jiru F, Skoch A, Wagnerova D, et al. The age dependence of T_2 relaxation times of N-acetyl aspartate, creatine and choline in the human brain at 3 and 4T. *NMR Biomed*. 2016;29(3):284-292. doi:10.1002/nbm.3456

6. Kirov II, Fleysher L, Fleysher R, Patil V, Liu S, Gonen O. Age dependence of regional proton metabolites T_2 relaxation times in the human brain at 3 T. *Magn Reson Med*. 2008;60(4):790-795. doi:10.1002/mrm.21715

7. Marjańska M, Emir UE, Deelchand DK, Terpstra M. Faster metabolite 1H transverse relaxation in the elder human brain. *PloS One*. 2013;8(10):e77572.

8. Brooks JCW, Roberts N, Kemp GJ, Gosney MA, Lye M, Whitehouse GH. A Proton Magnetic Resonance Spectroscopy Study of Age-related Changes in Frontal Lobe Metabolite Concentrations. *Cereb Cortex*. 2001;11(7):598-605. doi:10.1093/cercor/11.7.598

9. Christiansen P, Toft P, Larsson HBW, Stubgaard M, Henriksen O. The concentration of N-acetyl aspartate, creatine + phosphocreatine, and choline in different parts of the brain in adulthood and senium. *Magn Reson Imaging*. 1993;11(6):799-806. doi:10.1016/0730-725X(93)90197-L

10. Kreis R, Slotboom J, Hofmann L, Boesch C. Integrated data acquisition and processing to determine metabolite contents, relaxation times, and macromolecule baseline in single examinations of individual subjects. *Magn Reson Med*. 2005;54(4):761-768. doi:10.1002/mrm.20673

11. Nasreddine ZS, Phillips NA, Bédirian V, et al. The Montreal Cognitive Assessment, MoCA: A Brief Screening Tool For Mild Cognitive Impairment. *J Am Geriatr Soc*. 2005;53(4):695-699. doi:10.1111/j.1532-5415.2005.53221.x

12. Carson N, Leach L, Murphy KJ. A re-examination of Montreal Cognitive Assessment (MoCA) cutoff scores. *Int J Geriatr Psychiatry*. 2018;33(2):379-388. doi:10.1002/gps.4756

13. Ng KP, Chiew HJ, Lim L, Rosa-Neto P, Kandiah N, Gauthier S. The influence of language and culture on cognitive assessment tools in the diagnosis of early cognitive impairment and

dementia. *Expert Rev Neurother*. 2018;18(11):859-869. doi:10.1080/14737175.2018.1532792

14. Gong T, Hui SCN, Zöllner HJ, et al. Neurometabolic timecourse of healthy aging. *NeuroImage*. 2022;264:119740. doi:10.1016/j.neuroimage.2022.119740

15. Oeltzschner G, Zöllner HJ, Hui SC, et al. Osprey: Open-source processing, reconstruction & estimation of magnetic resonance spectroscopy data. *J Neurosci Methods*. 2020;343:108827.

16. Barkhuijsen H, De Beer R, Van Ormondt D. Improved algorithm for noniterative time-domain model fitting to exponentially damped magnetic resonance signals. *J Magn Reson 1969*. 1987;73(3):553-557.

17. Zöllner HJ, Považan M, Hui SC, Tapper S, Edden RA, Oeltzschner G. Comparison of different linear-combination modeling algorithms for short-TE proton spectra. *NMR Biomed*. 2021;34(4):e4482.

18. Hui SCN, Saleh MG, Zöllner HJ, et al. MRSCLOUD : A cloud-based MRS tool for basis set simulation. *Magn Reson Med*. 2022;88(5):1994-2004. doi:10.1002/mrm.29370

19. Simpson R, Devenyi GA, Jezzard P, Hennessy TJ, Near J. Advanced processing and simulation of MRS data using the FID appliance (FID-A)—An open source, MATLAB - based toolkit. *Magn Reson Med*. 2017;77(1):23-33. doi:10.1002/mrm.26091

20. Ashburner J, Barnes G, Chen CC, et al. SPM12 manual. *Wellcome Trust Cent Neuroimaging Lond UK*. 2014;2464:4.

21. Piechnik SK, Evans J, Bary LH, Wise RG, Jezzard P. Functional changes in CSF volume estimated using measurement of water T_2 relaxation. *Magn Reson Med*. 2009;61(3):579-586. doi:10.1002/mrm.21897

22. Daoust A, Dodd S, Nair G, et al. Transverse relaxation of cerebrospinal fluid depends on glucose concentration. *Magn Reson Imaging*. 2017;44:72-81. doi:10.1016/j.mri.2017.08.001

23. Spijkerman JM, Petersen ET, Hendrikse J, Luijten P, Zwanenburg JJM. T 2 mapping of cerebrospinal fluid: 3 T versus 7 T. *Magn Reson Mater Phys Biol Med*. 2018;31(3):415-424. doi:10.1007/s10334-017-0659-3

24. R Core Team. *R: A Language and Environment for Statistical Computing.* R Foundation for Statistical Computing; 2021. https://www.R-project.org/

25. RStudio Team. *RStudio: Integrated Development Environment for R*. RStudio, PBC; 2021. http://www.rstudio.com/

26. Benjamini Y, Hochberg Y. Controlling the False Discovery Rate: A Practical and Powerful Approach to Multiple Testing. *J R Stat Soc Ser B Methodol*. 1995;57(1):289-300. doi:10.1111/j.2517-6161.1995.tb02031.x

27. Murali-Manohar S, Gudmundson AT, Hupfeld KE, et al. *Metabolite T_1 Relaxation Times Differ across the Adult Lifespan*. Neuroscience; 2023. doi:10.1101/2023.01.06.522927

28. Ronen I, Valette J. Diffusion-Weighted Magnetic Resonance Spectroscopy. In: Harris RK, Wasylishen RL, eds. *eMagRes*. John Wiley & Sons, Ltd; 2015:733-750. doi:10.1002/9780470034590.emrstm1471

29. Dickstein DL, Kabaso D, Rocher AB, Luebke JI, Wearne SL, Hof PR. Changes in the structural complexity of the aged brain. *Aging Cell*. 2007;6(3):275-284. doi:10.1111/j.1474-9726.2007.00289.x

30. Verkerke M, Hol EM, Middeldorp J. Physiological and Pathological Ageing of Astrocytes in the Human Brain. *Neurochem Res*. 2021;46(10):2662-2675. doi:10.1007/s11064-021-03256-7

31. Jiang T, Cadenas E. Astrocytic metabolic and inflammatory changes as a function of age. *Aging Cell*. 2014;13(6):1059-1067. doi:10.1111/acel.12268

32. Peters A. The effects of normal aging on myelin and nerve fibers: A review. *J Neurocytol*. 2002;31(8/9):581-593. doi:10.1023/A:1025731309829

33. Safaiyan S, Kannaiyan N, Snaidero N, et al. Age-related myelin degradation burdens the clearance function of microglia during aging. *Nat Neurosci*. 2016;19(8):995-998. doi:10.1038/nn.4325

34. Knopman DS, Parisi JE, Salviati A, et al. Neuropathology of Cognitively Normal Elderly. *J Neuropathol Exp Neurol*. 2003;62(11):1087-1095. doi:10.1093/jnen/62.11.1087

35. Chad JA, Pasternak O, Salat DH, Chen JJ. Re-examining age-related differences in white matter microstructure with free-water corrected diffusion tensor imaging. *Neurobiol Aging*. 2018;71:161-170. doi:10.1016/j.neurobiolaging.2018.07.018

36. Hupfeld KE, Geraghty JM, McGregor HR, Hass CJ, Pasternak O, Seidler RD. Differential Relationships Between Brain Structure and Dual Task Walking in Young and Older Adults. *Front Aging Neurosci*. 2022;14:809281. doi:10.3389/fnagi.2022.809281

37. House MJ, St. Pierre TG, Kowdley KV, et al. Correlation of proton transverse relaxation rates (R_2) with iron concentrations in postmortem brain tissue from alzheimer's disease patients. *Magn Reson Med*. 2007;57(1):172-180. doi:10.1002/mrm.21118

38. Mitsumori F, Watanabe H, Takaya N. Estimation of brain iron concentration in vivo using a linear relationship between regional iron and apparent transverse relaxation rate of the tissue water at 4.7T. *Magn Reson Med*. 2009;62(5):1326-1330. doi:10.1002/mrm.22097

39. Schenker C, Meier D, Wichmann W, Boesiger P, Valavanis A. Age distribution and iron dependency of the T2 relaxation time in the globus pallidus and putamen. *Neuroradiology*. 1993;35(2):119-124. doi:10.1007/BF00593967

40. Tsai S, Posse S, Lin Y, et al. Fast mapping of the T_2 relaxation time of cerebral metabolites using proton echo-planar spectroscopic imaging (PEPSI). *Magn Reson Med*. 2007;57(5):859-865. doi:10.1002/mrm.21225

41. Träber F, Block W, Lamerichs R, Gieseke J, Schild HH. ^{1}H metabolite relaxation times at 3.0 tesla: Measurements of T1 and T2 values in normal brain and determination of regional

differences in transverse relaxation. *J Magn Reson Imaging*. 2004;19(5):537-545. doi:10.1002/jmri.20053

42. Wyss PO, Bianchini C, Scheidegger M, et al. In vivo estimation of transverse relaxation time constant (T_2) of 17 human brain metabolites at 3T: T_2 of 17 Human Brain Metabolites at 3T. *Magn Reson Med*. 2018;80(2):452-461. doi:10.1002/mrm.27067

43. Hetherington HP, Mason GF, Pan JW, et al. Evaluation of cerebral gray and white matter metabolite differences by spectroscopic imaging at 4.1T. *Magn Reson Med*. 1994;32(5):565-571. doi:10.1002/mrm.1910320504

44. An L, Li S, Shen J. Simultaneous determination of metabolite concentrations, T_1 and T_2 relaxation times. *Magn Reson Med*. 2017;78(6):2072-2081. doi:10.1002/mrm.26612

45. Mlynárik V, Gruber S, Moser E. Proton T_1 and T_2 relaxation times of human brain metabolites at 3 Tesla: METABOLITE T_1 AND T_2 IN HUMAN BRAIN AT 3 T. *NMR Biomed*. 2001;14(5):325-331. doi:10.1002/nbm.713

46. Deoni SCL, Peters TM, Rutt BK. High-resolution T_1 and T_2 mapping of the brain in a clinically acceptable time with DESPOT1 and DESPOT2. *Magn Reson Med*. 2005;53(1):237-241. doi:10.1002/mrm.20314

47. Schmitt P, Griswold MA, Jakob PM, et al. Inversion recovery TrueFISP: Quantification of T_1, T_2, and spin density. *Magn Reson Med*. 2004;51(4):661-667. doi:10.1002/mrm.20058

48. Fujita S, Hagiwara A, Hori M, et al. Three-dimensional high-resolution simultaneous quantitative mapping of the whole brain with 3D-QALAS: An accuracy and repeatability study. *Magn Reson Imaging*. 2019;63:235-243. doi:10.1016/j.mri.2019.08.031

49. Knight MJ, McCann B, Tsivos D, Couthard E, Kauppinen RA. Quantitative T1 and T2 MRI signal characteristics in the human brain: different patterns of MR contrasts in normal ageing. *Magn Reson Mater Phys Biol Med*. 2016;29(6):833-842. doi:10.1007/s10334-016-0573-0

50. Gudmundson AT, Koo A, Virovka A, et al. Meta-analysis and open-source database for in vivo brain Magnetic Resonance spectroscopy in health and disease. *Anal Biochem*. 2023;676:115227. doi:10.1016/j.ab.2023.115227

51. Tal A. The future is 2D : SPECTRAL-TEMPORAL fitting of dynamic MRS data provides exponential gains in precision over conventional approaches. *Magn Reson Med*. 2023;89(2):499-507. doi:10.1002/mrm.29456

52. Zöllner HJ, Davies-Jenkins C, Simicic D, Tal A, Sulam J, Oeltzschner G. Simultaneous multi-transient linear-combination modeling of MRS data improves uncertainty estimation. Published online November 4, 2023. doi:10.1101/2023.11.01.565164

53. Clarke WT, Ligneul C, Cottaar M, Ip IB, Jbabdi S. Universal dynamic fitting of magnetic resonance spectroscopy. *Magn Reson Med*. 2024;91(6):2229-2246. doi:10.1002/mrm.30001

619 54. Kirov II, Tal A. Potential clinical impact of multiparametric quantitative MR spectroscopy in
620 neurological disorders: A review and analysis. *Magn Reson Med*. 2020;83(1):22-44.
621 doi:10.1002/mrm.27912

622 55. Eylers VV, Maudsley AA, Bronzlik P, Dellani PR, Lanfermann H, Ding XQ. Detection of
623 Normal Aging Effects on Human Brain Metabolite Concentrations and Microstructure with
624 Whole-Brain MR Spectroscopic Imaging and Quantitative MR Imaging. *Am J Neuroradiol*.
625 2016;37(3):447-454. doi:10.3174/ajnr.A4557

626